

This is an Open Access document downloaded from ORCA, Cardiff University's institutional repository: <https://orca.cardiff.ac.uk/id/eprint/91912/>

This is the author's version of a work that was submitted to / accepted for publication.

Citation for final published version:

Perni, Stefano, Drexler, Sammy, Ruppel, Sergej and Prokopovich, Polina 2016. Lethal photosensitisation of bacteria using Silica-TBO nanoconjugates. *Colloids and Surfaces A: Physicochemical and Engineering Aspects* 510 , pp. 293-299. 10.1016/j.colsurfa.2016.06.022

Publishers page: <http://dx.doi.org/10.1016/j.colsurfa.2016.06.022>

Please note:

Changes made as a result of publishing processes such as copy-editing, formatting and page numbers may not be reflected in this version. For the definitive version of this publication, please refer to the published source. You are advised to consult the publisher's version if you wish to cite this paper.

This version is being made available in accordance with publisher policies. See <http://orca.cf.ac.uk/policies.html> for usage policies. Copyright and moral rights for publications made available in ORCA are retained by the copyright holders.



Lethal Photosensitisation of Bacteria Using Silica-TBO Nanoconjugates

by

Stefano Perni ¹, Sammy Drexler ^{1,#}, Sergej Ruppel ^{1,#}, Polina Prokopovich ^{1,*}

¹ School of Pharmacy and Pharmaceutical Sciences, Cardiff University, Cardiff, UK

[#] SD and SR contributed equally to the paper

* Corresponding author:

Dr. Polina Prokopovich e-mail: prokopovichp@cardiff.ac.uk

School of Pharmacy and Pharmaceutical Sciences

Cardiff University

Redwood Building, King Edward VII Avenue

Cardiff, UK

CF10 3NB

Tel: +44 (0)29 208 75820

Fax: +44 (0)29 208 74149

Abstract

Pathogenic microorganisms are gradually becoming resistant to antibiotics, thereby novel antimicrobial technology are urgently needed. Photodynamic therapy (PDT) is a process that employs the energy of photons to generate reactive oxygen species through a class a chemicals known as photosensitisers. PDT has shown antimicrobial activity as the oxygen reactive species can inactivate microorganisms, at the same time, the doses required to provide antimicrobial actions are not lethal to mammalian cells.

We covalently bound Toluidine blue O (TBO), a very common and safe photosensitiser, to silica nanoparticles. The conjugates exhibited antimicrobial activity against MRSA, *S. epidermidis* and *E. coli* when irradiated with laser light at 630 nm. Using a light source with a power of 500 mW the bacterial reduction exhibited a dose-response behaviour and it was $2 \log_{10}$ for *S. epidermidis* and *E. coli* after 2 and 3 min, respectively. No antimicrobial activity was exhibited by the unconjugated nanoparticles or by the laser light alone. The release of TBO from the nanoparticles was pH dependent with higher amounts of photosensitisers were detached at pH = 4 than pH = 7 consistent with the formation of amide bonds between nanoparticles and TBO.

The light activated nanoparticles developed in this work offer a platform for the controlled delivery of TBO through a pH responsive mechanism for antimicrobial applications.

1 Introduction

Non-antibiotic based antimicrobial therapies are an urgent need in the management of infections in light of the rising number of microorganisms exhibiting resistance to one or more antibiotics [1]. Skin and soft-tissue infections (SSTIs) caused by methicillin-resistant *Staphylococcus aureus* (MRSA) are very frequent and their rate has increased 20 folds in the last decade [2]; it has been estimated that every MRSA infection costs an extra 9000 £ to the NHS [3]. Despite the media focus on MRSA, numerous other pathogenic species have developed resistance, i.e. *Vancomycin-Resistant Enterococci* (VRE). SSTI incidence is 24.6 per 1000 person every year while among hospitalized patients the incidence is 7% to 10% [4]. The symptoms range from mild conditions, such as pyoderma, to serious life-threatening infections, such as necrotizing fasciitis. Microbial resistance can be originated by the cell altering the target of the drug without losing functionality (i.e. MRSA) through DNA mutations [5],[6].

The prevention and treatment of infections can be through antibiotic drugs or no antibiotic based techniques; cold gas plasma, metal nanoparticles and Photodynamic therapy (PDT) are examples of the technologies that do not employ antibiotics to inactivate microorganisms. Photodynamic therapy is a process based on the adsorption of photos by a photosensitizer (PS) and its transfer through a FRET (Förster resonance energy transfer) process (radiationless transfer of energy to neighbouring compound) to either oxygen (type 2 reaction) or other substrates (type 1 reaction). The energy adsorption by the PS induces its transition from the ground state to an excited state (singlet or triplet), from these unstable states the PS return to the ground state transferring energy to oxygen molecules forming reactive oxygen species (ROS) such as singlet oxygen ($^1\text{O}_2$) and other radicals (superoxide (O_2^\cdot) and OH^\cdot). ROS are then responsible for the oxidation of the substrate molecules [7]. Such potential cytotoxic activity of PDT has found applications in cancer treatments and as antimicrobial technique, so called antimicrobial PDT (aPDT); this has been possible because of the existence of biological safe PS (i.e. TBO, MB and indocyanine green) whose lethal dose to inactivate pathogenic microorganisms is smaller than mammalian cells [8],[9]. Another important benefit of aPDT is its efficacy against antibiotic resistant cells, broad spectrum of action and inability to induce further resistance in sensitive cells [10],[11]. All these virtues are due to the multi targets lethality mechanism of aPDT as ROS are unspecific in their interaction. The main applications of aPDT have been in dentistry [12] and dermatological set-ups [13], however, more recently, light activated materials have been

developed as self-cleaning/self-sterilising surfaces with possible applications in catheters and open surfaces [14]-[21].

As the threat posed by bacteria resistant to one or more antibiotics is a growing concern [22]-[25], the need for more effective antimicrobial techniques not based on antibiotic drugs i.e. aPDT is a pressing need.

Nanotechnology has been applied to aPDT in order to enhance the antimicrobial outcome [7],[26], for example PS have been encapsulated in nanoparticles to guide their penetration inside cells or they have been conjugated to nanocarriers to drive their accumulation close to the cell wall. Among the nanocarriers used as drug delivery systems, silica has been widely used because of the ease of production and biological compatibility. Silica nanoparticles based treatments have been developed in cancer [27] and antimicrobial applications [28],[29]. Silica nanoparticles loaded with antimicrobial compounds have been shown capable of reversing antibiotic resistance [29]-[32].

In this work, TBO, a very common photosensitiser, has been bound to silica nanoparticles previously functionalised to exhibit amino groups. The physical-chemical properties of the nanoconjugates have been characterised and the antimicrobial activity against examples of Gram+ (*S. epidermidis* and MRSA) and Gram- (*E. coli*) pathogens determined. Furthermore, the TBO release has been shown to be pH dependent.

2 Materials and methods

2.1 Chemicals

Toluidine Blue O (TBO), tetraethyl-orthosilicate (TEOS), 3-aminopropyltriethoxysilane (APTS), 2-(4-morpholino)-ethane sulfonic acid (MES), suberic acid bis-(N-hydroxy-succinimide ester), Triton X-100, NaOH, Sodium dodecyl sulfate (SDS), MTT (3-(4,5-dimethylthiazol-2yl)-2,5-diphenyltetrazolium bromide) Brain Heart Infusion (BHI) broth and Agar were purchased from Sigma-Aldrich. Ammonium hydroxide (29.6 %), cyclohexane, *n*-hexanol, isopropyl alcohol and methanol were purchased from Fisher Scientific. All chemicals were used as-received without further purification.

2.2 Synthesis silica-TBO nanoconjugates

Silica nanoparticles functionalised with amine groups ($\text{SiO}_2\text{-NH}_2$) were prepared in a one-pot synthesis by hydrolysis of TEOS in reverse microemulsion and subsequent surface functionalisation with amino groups [28]. Lastly, TBO molecules were covalently conjugated to the silica surface.

In a typical synthesis, 17.7 g of Triton (X-100) were mixed with 16 ml of *n*-hexanol, 75 ml of cyclohexane, and 4.8 ml of deionised water under vigorous stirring. Once the solution became transparent, 600 μl of ammonium hydroxide were added to the solution. The solution was subsequently sealed and stirred for 20 min, followed by addition of 1 ml of TEOS and stirring for 24 h. The silica nanoparticles surface was functionalised with amine groups adding 50 μl of APTS to the microemulsion under stirring and incubating for further 24 hours. The silica surface functionalised particles, denoted $\text{SiO}_2\text{-NH}_2$, were then recovered by adding ethanol (200 ml) to break the microemulsion and centrifuging at 14000 rpm for 10 min (LE-80K Ultracentrifuge, Beckman Coulter, UK) at 20 °C; the nanoparticles were then rigorously washed with methanol.

The conjugation of TBO to $\text{SiO}_2\text{-NH}_2$ nanoparticles was carried out as follows: 50 mg of TBO were dissolved in 100 ml of MES buffer (0.1 M, pH 6.0); this solution was used to disperse 250 mg of $\text{SiO}_2\text{-NH}_2$ and, finally, 50 mg of suberic acid bis-(*N*-hydroxysuccinimide ester) were added. The suspension was kept under vigorous mixing for 24 hours at room temperature in the dark and the conjugates were recovered centrifuging at 14000 rpm for 10 min (LE-80K Ultracentrifuge, Beckman Coulter, UK) at 20 °C. The silica-TBO conjugates were washed three times in methanol and left to dry in the dark.

2.3 Silica-TBO nanoconjugates characterisation

Size and shape of the conjugates were determined through transmission electron microscopy (TEM); 4 μl droplet of conjugates suspension were deposited on a plain carbon-coated copper TEM grid, water was evaporated under ambient laboratory conditions for several hours. Bright field TEM images were obtained using a TEM (Philips CM12, FEI Ltd, UK) operating at 80kV fitted with an X-ray microanalysis detector (EM-400 Detecting Unit, EDAX UK) utilising EDAX's Genesis software. Images (magnification of the images was $\times 100,000$) were recorded using a SIS MegaView III digital camera (SIS Analytical, Germany) and analysed with ImageJ; the diameter of at least 100 particles was determined.

Fourier-Transformed Infrared spectra (FTIR) of the samples were collected with Perkin Elmer Spectrum One with Ge/Ge UATR (wavenumber from 4000 to 600 cm^{-1}).

Thermogravimetric analysis (TGA) was performed using a Stanton Redcroft, STA-780 series TGA; data were recorded from 25 to 800 $^{\circ}\text{C}$ with a constant heating rate of 10 $^{\circ}\text{C min}^{-1}$.

2.4 Antimicrobial activity of Si-TBO nanoconjugates

The bacteria used in this study were *E. coli* (NCTC10418), methicillin-resistant *Staphylococcus aureus* MRSA (NCTC12493) and *S. epidermidis* (ATCC12228). They were stored at -80°C ; when needed they were plated on BHI agar and incubated for 24 hours at 37°C . The plates were then kept at 4°C for no more than 2 weeks. 10 ml of fresh sterile BHI broth in a 15 ml tube were inoculated with a loopful of cells from a single colony on a BHI plate; after incubating statically for 24 hours at 37°C the cells suspension was diluted with sterile PBS 1:100. This cells suspension was used to disperse the Si-TBO conjugates to a concentration of 10 mg/ml; 200 μl of this suspension were immediately poured in a 96 wells plate. The well was irradiated with the light (633 nm) from a 500 mW laser (BFi Optilas Ltd, UK) for 0.5, 1, 2 and 3 min; energy density (40 mW/mm^2). After exposure, the bacterial cells (L+S+) were counted through serial dilutions in sterile PBS and plating on BHI Agar (plates were incubated 24 hours at 37°C). Along this test (L+S+), control experiments were performed counting cells that were exposed, for the same length of time, to laser light without conjugates (L+S-). Cells were also stored in the dark with (L-S+) and without the silica conjugates (L-S-). The tests were performed on three independent cultures on conjugates from three independent batches.

Additionally, a TBO solution 30 mg/ml was prepared in PBS and filter sterilised; this solution was diluted using the bacterial suspensions (10^6 CFU/ml in PBS) prepared as described above to a final concentration of TBO of 300 mg/l. 200 μl of this suspension was immediately poured in a 96 wells plate. The well was irradiated with the light (633 nm) from a 500 mW laser (BFi Optilas Ltd, UK) for 0.5, 1, 2 and 3 min; energy density (40 mW/mm^2). After exposure the bacterial cells (L+S+) were counted through serial dilutions in sterile PBS and plating on BHI Agar (plates incubated 24 hours at 37°C). The tests were performed on three independent cultures.

2.5 Bacterial uptake of TBO

10 mL of fresh sterile BHI broth were inoculated with a loopful of cells from a single colony on a BHI plate and incubated aerobically for 24 h at 37°C statically. The bacterial suspension was then centrifuged with an Avanti J-20XP Centrifuge (Beckmann and Coulter, United States) for 3 min at 2938 g, afterwards the supernatant was disposed. After one wash with PBS and centrifugation (3 min at 2938 g), 1 mL of Si-TBO suspension in PBS (10 mg/ml) or pure TBO (300 mg/l) was added to the precipitated cells. The resulting solution was vortexed and incubated 3 min at 37°C statically. The suspension was passed through a filter with 0.45 µm pores to separate the cells from the particles. The filter was washed in PBS and the cells centrifuged (3 min at 2938 g).

After discharging the supernatant, the cells were dissolved in 1 mL 0.1 M NaOH/1% Sodium dodecyl sulfate (SDS) and incubated at 37°C for 24 h to lyase the cells and release the TBO. The optical density of samples was measured at a 650 nm using a plate reader (Labtech LT5000MS) against a calibration curve prepared using the corresponding bacterial lysate.

The protein content of the entire cell extracts was determined for each culture by a modified Lowry method using bovine serum albumin (BSA) dissolved in 0.1 M NaOH/1% SDS to construct calibration curves. The tests were performed on three independent cultures and results are expressed as nmol of TBO/mg of cell protein.

2.6 Cytocompatibility of Si-TBO nanoconjugates

Human fibroblasts (MRC-5) were cultured in RPMI-1640 medium supplemented with glutamine, 10% FBS and 1% pen-strep, in a humidified incubator at 37 °C and 5% CO₂. When about 70% confluence was reached, fibroblasts were washed in sterile PBS and trypsinated. 96 well plates were the inoculated with approximately 6000 cells/well in 200 µl of media, plates were incubated in a humidified incubator at 37 °C and 5% CO₂. After 2 days the medium was removed and cells were washed in sterile PBS; 200 µl of Si-TBO conjugates suspension in PBS at a concentration of 10 mg/ml were poured in a 96 wells plate. The well was irradiated with the light (633 nm) from a 500 mW laser (BFi Optilas Ltd, UK) for 3 min; energy density (40 mW/mm²) (L+S+) or kept in the dark for the same length of time (L-S+). Control samples were also

prepared adding 200 μ l of pure sterile PBS to the wells and either irradiated (L+S-) or kept in the dark (L-S-).

Fibroblast viability was assessed through MTT (3-(4,5-dimethylthiazol-2-yl)-2,5-diphenyltetrazolium bromide) assay. After exposure to laser or storage in the dark the suspension in the wells was replaced with phenol red-free medium and 50 μ l of MTT stock solution (5 mg/ml) was added to each well and incubated at 37°C in humidified atmosphere containing 5% CO₂ for 4 hour. The metabolised MTT, formazan, was re-suspended with 50 μ l of dimethyl sulfoxide (DMSO). 200 μ l were transferred to a 96-well plate absorbance at 560 nm was read using a spectrophotometer (ELISA Reader Labtech LT-5000MS). All experiments were performed in triplicates.

2.7 TBO release from conjugates

TBO release was quantified dispersing conjugates (5 mg) in citric acid - Na₂HPO₄ buffers pH = 7, 6, 5 and 4 (1 ml); the suspension was incubated at 37 °C in Eppendorfs. At prefixed times, the suspension was centrifuged at 5087 g (Multifuge 3 S-R, Heraeus) for 5 min and samples were taken (200 μ l) from the supernatant. TBO in the buffer was quantified through adsorption at 630 nm (FLUOROstar Optima, BMG labtech); standards of known TBO in each buffer were also analysed simultaneously to provide pH-dependent calibration. After analysis the samples were added back to the original Eppendorf and the nanoparticles suspended. The tests were performed in duplicates on conjugates from three independent batches.

3 Results and discussion

3.1 Conjugates characterisation

The synthesis of the silica nanoparticles was carried out using the widely employed Stöber method that is based on the hydrolysis of TEOS in an alkaline solution [33]. The silica unconjugated nanoparticles (SiO₂-NH₂) were roundly shaped as seen in TEM images (Figure 2a) and the diameter was narrowly distributed (57 ± 9 nm) as seen in Figure 2b; the conjugation of TBO did not have impact on the shape (Figure 2c) and diameter of the nanoparticles (Figure 2d) that was 59 ± 7 nm.

The Stober process allows the formation of silica nanoparticles of a wide size range 2 to 2000 nm through the control of the reaction conditions [34]; we employed parameters similar to Guo et al. 2010 [28] that reported the formation of nanoparticles with diameter ranging from 50 to 80 nm, very close to our results. The FTIR spectra in Figure 3 showed strong adsorption peaks at about 1100 cm^{-1} for all the nanoparticles; these are related to Si-O-Si stretching vibration of silanol groups. The presence of $-\text{CH}_2$ groups was confirmed by C-H stretching at 2926 cm^{-1} and C-H scissoring vibration at 1456 cm^{-1} . N-H stretching is responsible for the peaks between 3200 and 3400 cm^{-1} confirming the presence of NH_2 on the silica functionalised nanoparticles. These FTIR spectra are similar to those presented by Li et al. 2012 [35]. Moreover, the FTIR spectra did not show evidence of TBO on the surface (Figure 3) and this was probably connected to the low amount of dye bound on the surface.

Both type of nanoparticles (unconjugated and conjugated) started to lose mass when heated at about 200°C consistent with the oxidation of organic matter present. The unconjugated particles exhibited a lower mass reduction (about 8%) than the conjugated at 800°C when it can be assumed that only the inorganic fraction of the nanoparticles is left. The TBO load on the nanoparticles was determined as the difference between the organic fraction of unconjugated and conjugated samples, this was estimated to be around 3-4 % w/w. Similar loads on nanoparticles through conjugation on the surface of functionalised nanoparticles were reported in other works [36]-[38].

3.2 Photosensitisation of bacteria and fibroblasts

The number of viable cells of *E. coli*, MRSA and *S. epidermidis* exposed to laser light in the presence of Si-TBO nanoparticles decreased with increasing exposure time (Figure 5). After 3 min of laser irradiation, *E. coli* exhibited a reduction of about $2\log_{10}$ whilst *S. epidermidis* returned the same level of inactivation after a shorter period of irradiation (2 min), when the irradiation was conducted for 3 min the number of viable cells fell below the detection limit. Also the number of viable MRSA cells after laser irradiation in the presence of the silica-TBO nanoconjugates decreased with increasing treatment time; generally the inactivation of MRSA was lower than *S. epidermidis* and greater than *E. coli*. Moreover, for all three bacterial species tested, the inactivation resulting from the exposure to pure TBO (at a concentration equivalent to that of silica-TBO nanoconjugates) was lower than in the case of silica-TBO nanoconjugates for analogous irradiation times (Figure 5).

For all three bacterial species no inactivation was detected when cells were exposed to laser light without the presence of Si-TBO nanoparticles (L+S-) or when in contact with the nanoparticles without irradiation (L-S+) demonstrating the non bactericidal activity of either the laser or the nanoparticles individually but the necessary synergistic interaction. These results are the common pattern in aPDT and are the consequence of the physical mechanism of PDT (the interaction between photons and photosensitisers) and also highlight the lack cytotoxicity of the Si-TBO nanoparticles developed in this work. Furthermore, the greater resistance to aPDT inactivation found in this work for *E. coli* compared to *S. epidermidis* and MRSA is in agreement with the relatively well known lower susceptibility of Gram- bacteria to this technology than Gram+ that has been linked to the different cell wall structure characterising these two classes of bacteria. The species used in this work were chosen as they are common representative of pathogens present on the skin [39] and routinely employed to test sanitation processes.

The amount of TBO found inside the bacterial cells increased when the nanocojugates were employed (Figure 7) compared to exposure to the corresponding amount of dye in its free form. Moreover, Gram+ bacteria uptake of the dye was higher than *E. coli*; this can be attributed to the different cell wall structure that is well known to reduce Gram- staining. The higher inactivation kinetics of the two Gram+ positive species tested than *E. coli* (Gram-) is linked to the different uptake of the dye; in addition our results suggest that the improved lethality observed for the Si-TBO nanoconjugates could be a consequence of the enhanced cell uptake of the photosensitiser. It has been suggested that local concentrations of antimicrobial agents, through the conjugation on nanoparticles surfaces, is a method to enhance antimicrobial efficacy focusing the activity in locations close or inside cells; this spatial disuniformity could only be achieved through drug delivery systems otherwise molecules would uniformly distribute [30],[40],[41].

The Si-TBO nanoconjugates prepared in this work did not impact on fibroblasts viability either in the dark or in conjunction with laser irradiation for 3 min (Figure 6), demonstrating that the Si-TBO nanoconjugates did not present cytotoxic properties towards mammalian cells, at least for the laser irradiation time sufficient to inactivate pathogenic bacteria. It is well established that mammalian cells are generally more resistant to the ROS produced by PDT than bacteria [8],[9]; this provides the foundation for aPDT as treatments are dosed to provide bacteria killing but not to result in mammalian cells damage. Our results were expected and they are in agreement with the established knowledge.

3.3 pH dependent photosensitiser release from conjugates

TBO was released from the conjugated when in contact with a liquid phase (Figure 8). The amount of TBO released increased with time following a Fickian profile; the pH of the buffer was critical in determining the kinetic, the more acidic pH gave quicker release than the neutral; no statistical difference was recorded between pH = 5 and 6. The concentration of TBO in the buffer containing Si-TBO continued increasing TBO for at least 48 hours in case of acid condition, whilst did not increase after the first 4 hours for neutral conditions.

The conjugation of TBO to the silica nanocarriers is performed through the formation of an amide bond; therefore, it was expected that acidic condition would favour the hydrolysis of this link hence increasing the TBO release. Additionally, the amount of photosensitiser detached from the carriers at neutral pH was very small highlighting the strength of the bond formed.

Silica nanoparticles loaded with photosensitiser can be prepared also through the direct entrapment of the dye inside the nanoparticles during the synthesis [42], however such approach leads to a very quick release of the light activated compound in a pH uncontrolled manner.

4 Conclusions

We photoactivated silica nanoparticles through binding TBO to the previously functionalised nanoparticles, these conjugates exhibit pH responsive release of the photosensitisers and antimicrobial activity when irradiated. The enhanced antimicrobial activity of the Si-TBO nanoconjugates, following laser irradiation, appeared correlated to increased bacterial cell uptake of the dye.

These conjugates can be employed to prepare materials such as hydrogels and topical creams that exhibit light dependant antimicrobial activity; moreover the use of silica supported TBO, instead of the free drug, enables the formulation of nanocomposites with enhanced mechanical properties accompanying the light activated antimicrobial activity and provides a pH responsive drug delivery system.

5 References

- [1] <http://bsac.org.uk/news/antimicrobial-resistance-poses-catastrophic-threat-says-chief-medical-officer/#sthash.qAnzQx3C.dpuf>
- [2] C.R. Frei, B.R. Makos, K.R. Daniels, C.U. Oramasionwu. Emergence of community-acquired methicillin-resistant *Staphylococcus aureus* skin and soft tissue infections as a common cause of hospitalization in United States children. *J. Pediatr. Surg.* 45 (2010) 1967-1974
- [3] <http://www.telegraph.co.uk/news/uknews/2194132/Every-MRSA-case-costs-NHS-an-extra-9000.html>
- [4] V. Ki, C. Rotste. Bacterial skin and soft tissue infections in adults: A review of their epidemiology, pathogenesis, diagnosis, treatment and site of care. *Can. J. Infect. Dis. Med. Microbiol.* 19 (2008) 173-184
- [5] P.D. Stapleton, P.W. Taylor. Methicillin resistance in *Staphylococcus aureus* mechanisms and modulation. *Sci. Prog.* 85(1) (2002) 57-72
- [6] S.W. Wu, H. de Lencastre, A. Tomasz. Recruitment of the *mecA* gene homologue of *Staphylococcus sciuri* into a resistance determinant and expression of the resistant phenotype in *Staphylococcus aureus*. *J. Bacteriol.* 183(8) (2001) 2417-2424
- [7] S. Perni, P. Prokopovich, J. Pratten, I.P. Parkin, M. Wilson. Nanoparticles: Their Potential Use in Antibacterial Photodynamic Therapy. *Photochem. Photobiol. Sci.* 10 (2011) 712-720
- [8] B. Zeina, J. Greenman, D. Corry, W.M. Purcell. Cytotoxic effects of antimicrobial photodynamic therapy on keratinocytes in vitro. *Br. J. Dermatol.* 146(4) (2002) 568-573
- [9] B. Zeina, J. Greenman, D. Corry, W.M. Purcell. Antimicrobial photodynamic therapy: assessment of genotoxic effects on keratinocytes in vitro. *Br. J. Dermatol.* 148(2) (2003) 229-232
- [10] F. Giuliani, A.C. Martinelli, D. Arbia, L. Fantetti and G. Roncucci. In Vitro Resistance Selection Studies of RLP068/Cl, a New Zn(II) Phthalocyanine Suitable for Antimicrobial Photodynamic Therapy. *Antimicrob. Agents Chemother.* 54(2) (2010) 637-642
- [11] A. Tavares, C.M.B. Carvalho, M.A. Faustino, G.P.M.S. Neves, J.P.C. Tomé, A. C. Tomé, J.A.S. Cavaleiro, A. Cunha, N.C.M. Gomes, E. Alves, E. Almeida. Antimicrobial Photodynamic Therapy: Study of Bacterial Recovery Viability and Potential Development of Resistance after Treatment. *Mar. Drugs* 8 (2010) 91-105
- [12] M. Wilson. Lethal photosensitisation of oral bacteria and its potential application in the photodynamic therapy of oral infections. *Photochemical and Photobiological Sci.* 3(5) (2004) 412-418
- [13] M.R. Hamblin, T. Hasan. Photodynamic therapy: a new antimicrobial approach to infectious disease? *Photochem Photobiol Sci.* 3(5) (2004) 436-450
- [14] S. Ismail, S. Perni, J. Pratten, I.P. Parkin, M. Wilson. Clinical Efficacy of Novel Light-activated Antimicrobial Coating for Disinfecting Hospital Surfaces. *Infect. Control Hosp. Epidemiol.* 32(11) (2011) 1130-1132
- [15] S. Perni, C. Piccirillo, P. Prokopovich, J. Pratten, I.P. Parkin, M. Wilson. Antimicrobial Properties of Light-Activated Polyurethane Containing Indocyanine Green. *J. Biomed. Appl.* 25 (2011) 387-400
- [16] S. Perni, P. Prokopovich, I.P. Parkin, M. Wilson, J. Pratten. Prevention of Biofilm Accumulation on a Light-activated Antimicrobial Catheter Material. *J. Mater. Chem.* 20(39) (2010) 8668-8673
- [17] S. Perni, C. Piccirillo, A. Kafizas, M. Uppal, J. Pratten, M. Wilson, I.P. Parkin. Antibacterial Activity of Silicone Containing Methylene Blue and Gold Nanoparticles of Various Sizes Under Laser Light Irradiation. *J. Cluster Sci.* 21(3) (2010) 427-438

- [18] P. Prokopovich, S. Perni, C. Piccirillo, J. Pratten, I.P. Parkin, M. Wilson. Frictional Properties of Light-Activated Silicone and Polyurethane Against Blood Vessels. *J. Mater. Sci. Mater. Med.* 21(2) (2010) 815-821
- [19] C. Piccirillo, S. Perni, J. Gil-Thomas, P. Prokopovich, M. Wilson, J. Pratten, I.P. Parkin. Antibacterial Activity of Methylene Blue and Toluidine Blue O Covalently Bounded to Modified Silicone Polymer Surface. *J. Mater. Chem.* 19(34) (2009) 6167-6171
- [20] S. Perni, P. Prokopovich, C. Piccirillo, J.R. Pratten, I.P. Parkin, M. Wilson. Toluidine Blue-Containing Polymers Exhibit Bactericidal Activity When Irradiated with Red Light. *J. Mater. Chem.* 19(17) (2009) 2715-2723
- [21] S. Perni, C. Piccirillo, J.R. Pratten, P. Prokopovich, W. Chrzanowski, I.P. Parkin, M. Wilson. The Antimicrobial Properties of Light-activated Polymers Containing Methylene Blue and Gold Nanoparticles. *Biomaterials* 30(1) (2009) 89-93
- [22] H.C. Neu. The Crisis in Antibiotic Resistance. *Science* 257: (1992) 1064-1073.
- [23] FY15 Detect and Protect Against Antibiotic Resistance Budget Initiative, Centers for Disease Control and Prevention: Atlanta, GA, 2003,
<http://www.cdc.gov/drugresistance/threat&report&2013/pdf/FY15&DPAR&budget&init.pdf>
- [24] B. Spellberg, J.H. Powers, E.P. Brass, L.G. Miller, J.E. Edwards. Trends in Antimicrobial Drug Development: Implications for The Future. *Clin. Infect. Dis.* 38 (2004) 1279-12864
- [25] A.J. Alanis. Resistance to Antibiotics: Are We in the Post Antibiotic Era? *Arch. Med. Res.* 36 (2005) 697-705
- [26] D. Bechet, P. Couleaud, C. Frochot, M.L. Viriot, F. Guillemin, M. Barberi-Heyob. Nanoparticles as vehicles for delivery of photodynamic therapy agents. *Trends Biotechnol.* 26(11) (2008) 612-621
- [27] P. Couleaud, V. Morosini, C. Frochot, S. Richeter, L. Raehm, J.O. Durand. Silica-based nanoparticles for photodynamic therapy applications. *Nanoscale* 2(7) (2010) 1083-1095
- [28] Y. Guo, S. Rogelj, P. Zhang. Rose Bengal Decorated Silica Nanoparticles as Photosensitizers for Inactivation of Gram Positive Bacteria. *Nanotech.* 21 (2010) 065102
- [29] L.B. Capeletti, L.F. de Oliveira, K. de A. Gonçalves, J.F. de Oliveira, A. Saito, J. Kobarg, J.H. dos Santos, M.B. Cardoso. Tailored silica-antibiotic nanoparticles: overcoming bacterial resistance with low cytotoxicity. *Langmuir* 30(25) (2014) 7456-7464
- [30] L. Wang, Y.P. Chen, K.P. Miller, B.M. Cash, S. Jones, S. Glenn, B.C. Benicewicz, A.W. Decho. Functionalised nanoparticles complexed with antibiotic efficiently kill MRSA and other bacteria. *Chem. Commun.* 50(81) (2014) 12030-12033
- [31] D. Şen Karaman, S. Sarwar, D. Desai, E.M. Björk, M. Odén, P. Chakrabarti, J.M. Rosenholma, S. Chakraborti. Shape engineering boosts antibacterial activity of chitosan coated mesoporous silica nanoparticle doped with silver: a mechanistic investigation. *J. Mater. Chem. B* 4 (2016) 3292-3304
- [32] S. Agnihotri, R. Pathak, D. Jha, I. Roy, H.K. Gautam, A.K. Sharma, P. Kumar. Synthesis and antimicrobial activity of aminoglycoside-conjugated silica nanoparticles against clinical and resistant bacteria. *New J. Chem.* 39 (2015) 6746-6755
- [33] W. Stöber, A. Fink, E. Bohn. Controlled growth of monodisperse silica spheres in the micron size range. *J. Colloid Interface Sci.* 26 (1968) 62-69
- [34] K. Nozawa, H. Gailhanou, L. Raison, P. Panizza, H. Ushiki, E. Sellier, J.P. Delville, M.H. Delville. Smart control of monodisperse Stöber silica particles: effect of reactant addition rate on growth process. *Langmuir* 21(4) (2005) 1516-1523
- [35] W. Li, Y. Xu, Y. Zhou, W. Ma, S. Wang, Y. Dai. Silica nanoparticles functionalized via click chemistry and ATRP for enrichment of Pb(II) ion. *Nanoscale Res. Lett.* 7(1) (2012) 485

- [36] J. Gil-Thomas, S. Tubby, I. P. Parkin, N. Narband, L. Dekker, S. P. Nair, M. Wilson and C. Street, Lethal Photosensitisation of *Staphylococcus aureus* Using a Toluidine Blue O–Tiopronin–Gold Nanoparticle Conjugate. *J. Mater. Chem.* 17 (2007) 3739-3746
- [37] J. Gil-Thomas, L. Dekker, N. Narband, I. P. Parkin, S. P. Nair, C. Street, M. Wilson. Lethal photosensitisation of bacteria using a tin chlorin e6–glutathione–gold nanoparticle conjugate. *J. Mater. Chem.* 21 (2011) 4189-4196
- [38] S. Perni, P. Prokopovich. Continuous Release of Gentamicin from Gold Nanocarriers. *RSC Advances* 4 (2014) 51904-51910
- [39] M. Otto. *Staphylococcus epidermidis* - the 'accidental' pathogen". *Nature Rev. Microbiol.* 7(8) (2009) 555-567
- [40] H. Zhu, Q. Geng, W. Chen, Y. Zhu, J. Chen, J. Du. Antibacterial high-genus polymer vesicle as an “armed” drug carrier. *J. Mater. Chem. B* 1 (2013) 5496-5504.
- [41] C. Zhang, Y. Zhu, C. Zhou, W. Yuan, J. Du. Antibacterial vesicles by direct dissolution of a block copolymer in water. *Polym. Chem.* 4 (2013) 255-259
- [42] He X, Wu X, Wang K, Shi B, Hai L. Methylene blue-encapsulated phosphonate-terminated silica nanoparticles for simultaneous in vivo imaging and photodynamic therapy. *Biomaterials* 2009;30(29):5601-5609

Figure captions

Figure 1. Reaction scheme of the preparation of silica nanoparticles and TBO conjugation.

Figure 2. Example of TEM image (a) and size distribution (b) of Silica nanoparticles before TBO conjugation and after TBO binding (c and d).

Figure 3. Fourier Transformed Infrared spectra (FTIR) of silica conjugates from 4000 to 600 cm^{-1} .

—— TBO ——— SiO₂-TBO — — SiO₂-NH₂

Figure 4. Mass loss during Thermal Gravimetric Analysis (TGA) of Silica nanoparticles and silica photosensitiser conjugates.

—— SiO₂-NH₂ ——— SiO₂- TBO

Figure 5. Time dependent antimicrobial activity of Silica-TBO conjugates against (a) *E. coli* and (b) *S. epidermidis* and MRSA (c) after exposure to red laser (630 nm).

● L+S+ ○ L+S- ▼ L-S+ △ L-S- ■ L+ pure TBO

Figure 6. Viability of fibroblast determined using MTT assay after exposure to Si-TBO nanoconjugates and red laser irradiation.

Figure 7. Bacterial cells uptake of TBO using either Si-TBO nanoconjugates (grey columns) or an equivalent photosensitisers amount in pure form (black columns).

Figure 8. Release profiles of TBO from SiO₂-TBO nanoconjugates in buffers of various pH.

● pH = 4 ○ pH = 5 ▼ pH = 6 △ pH = 7

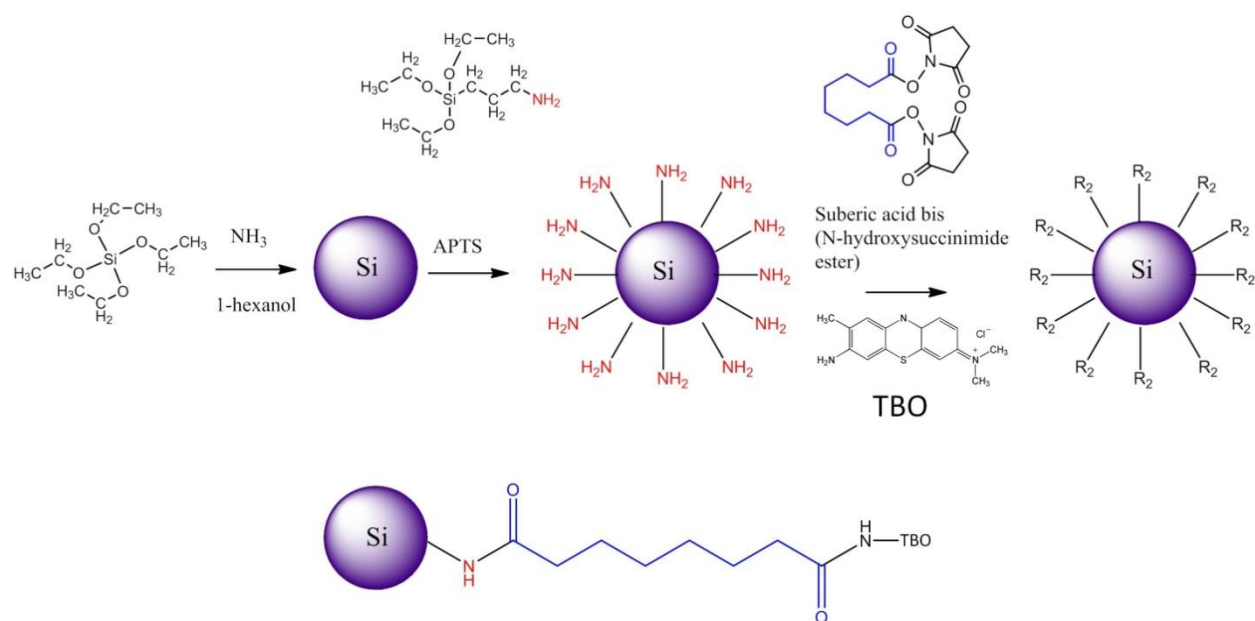


Figure 1

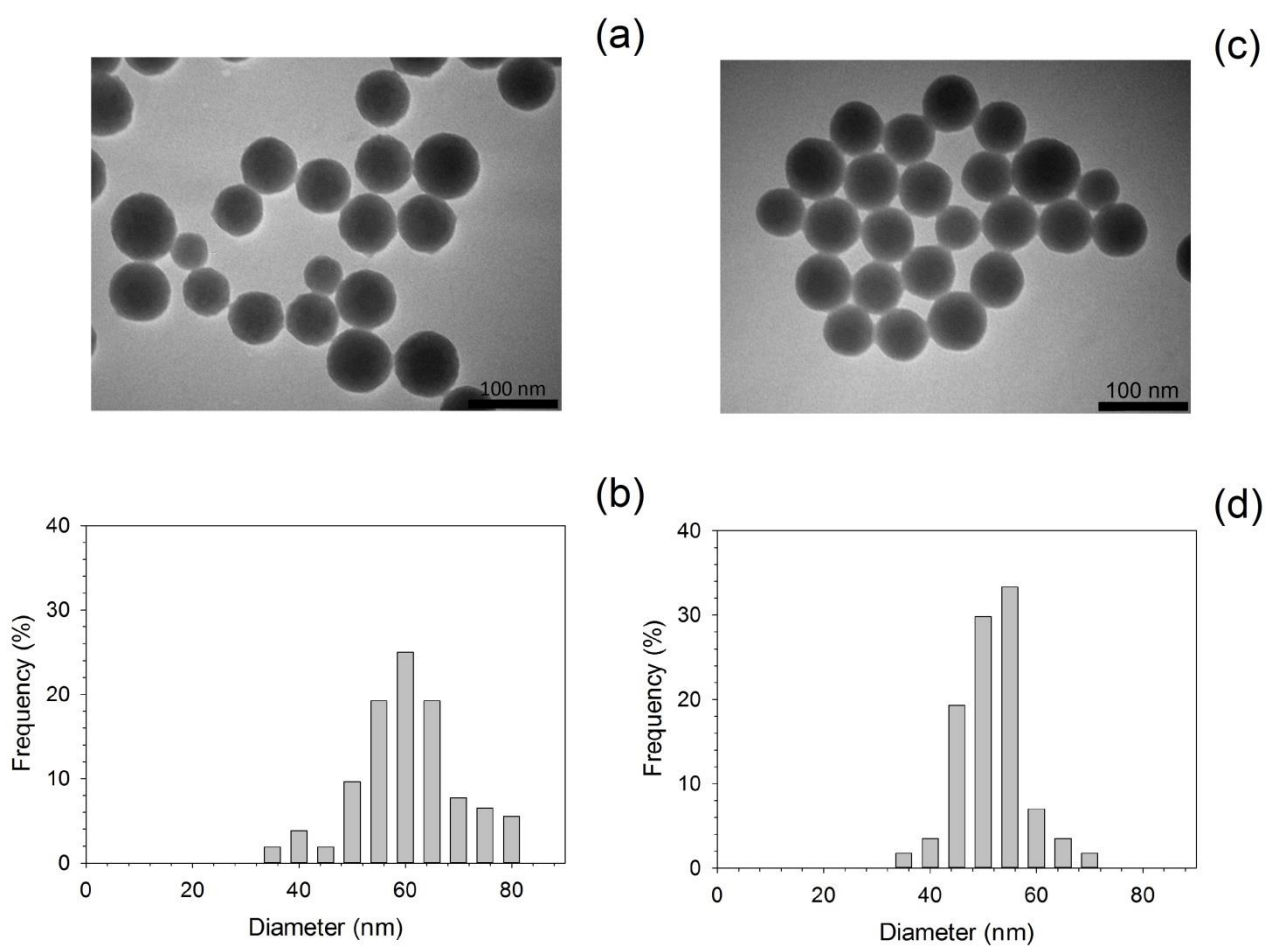


Figure 2

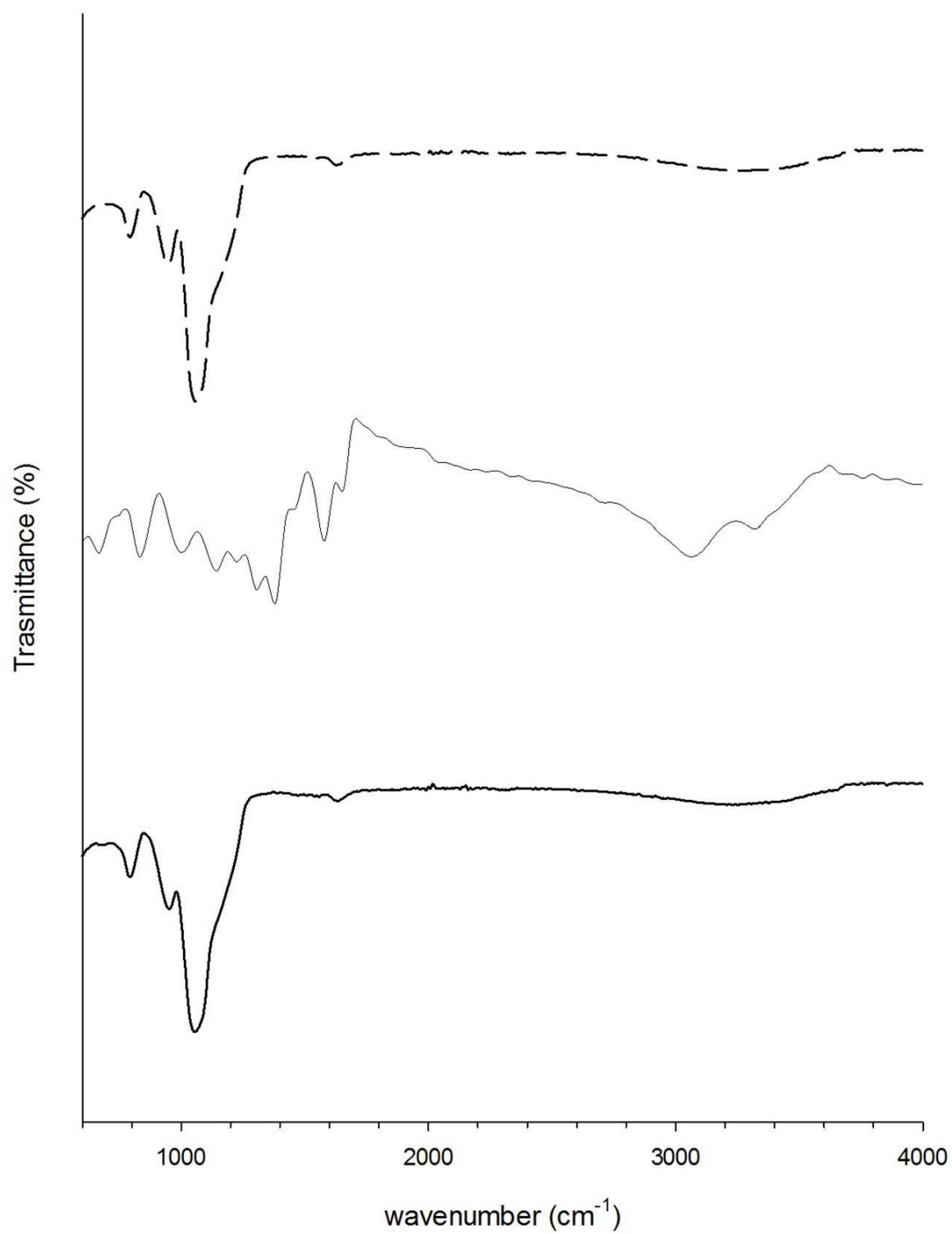


Figure 3

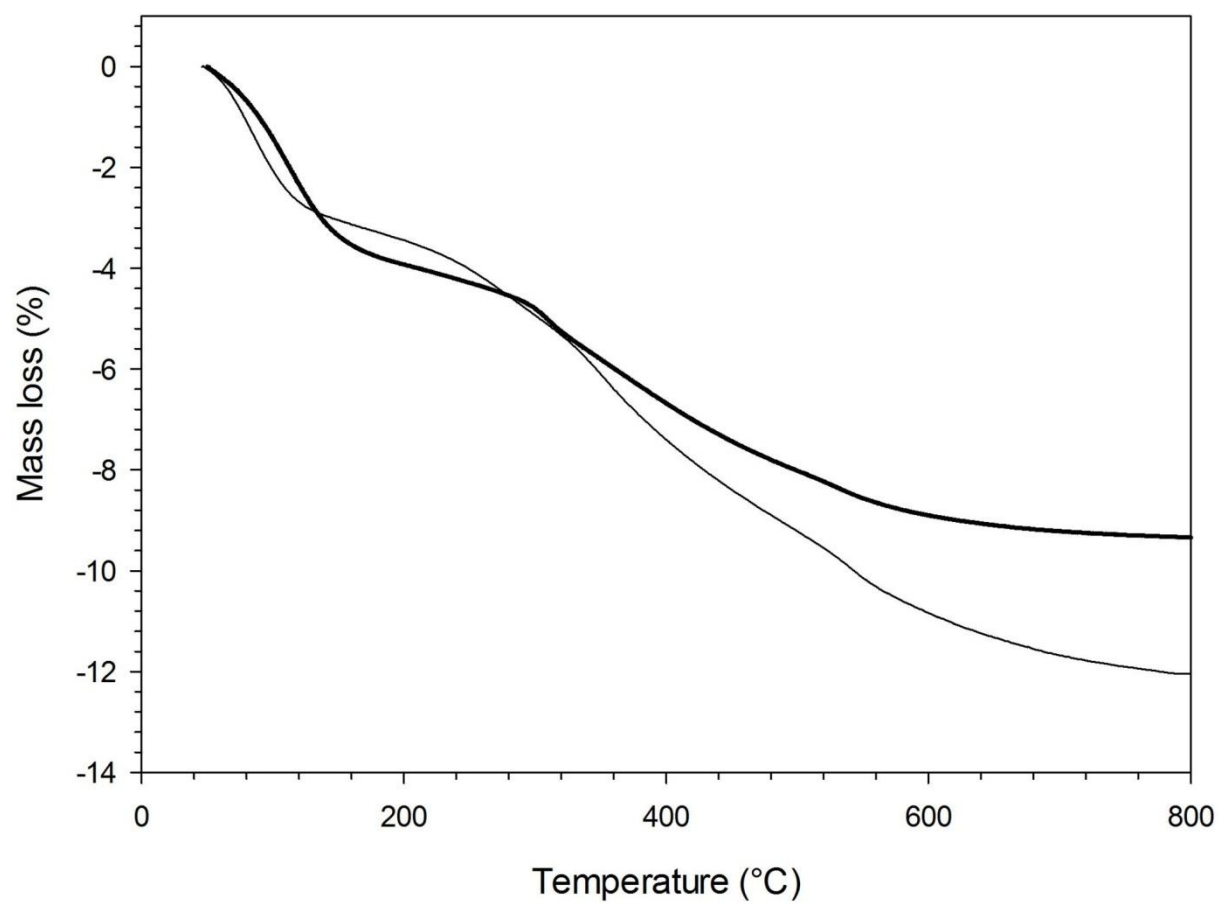


Figure 4

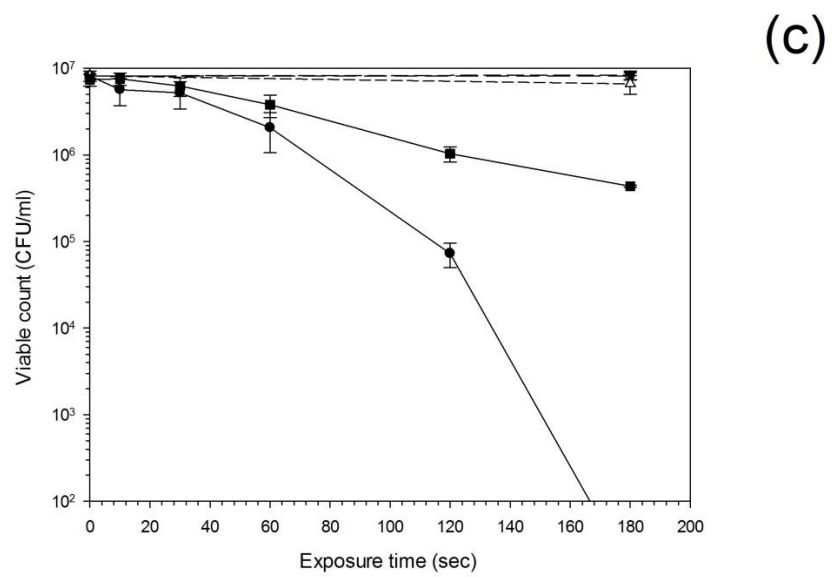
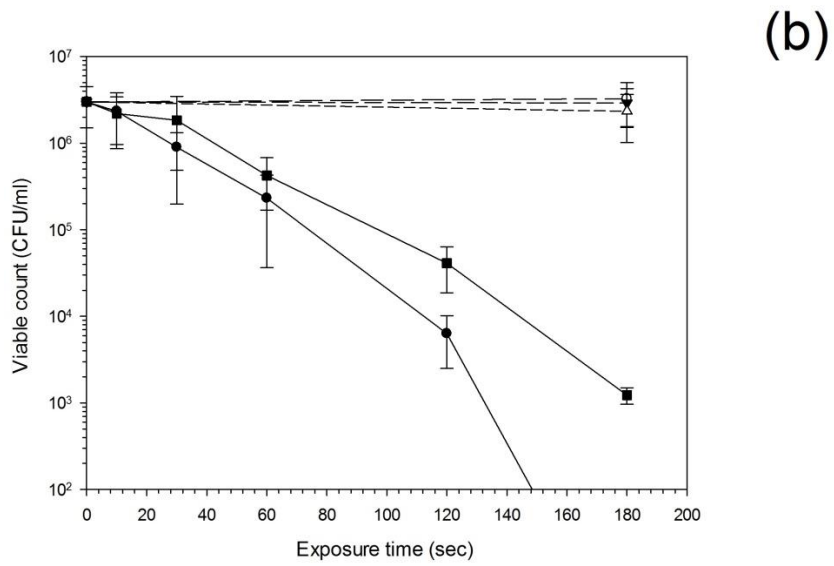
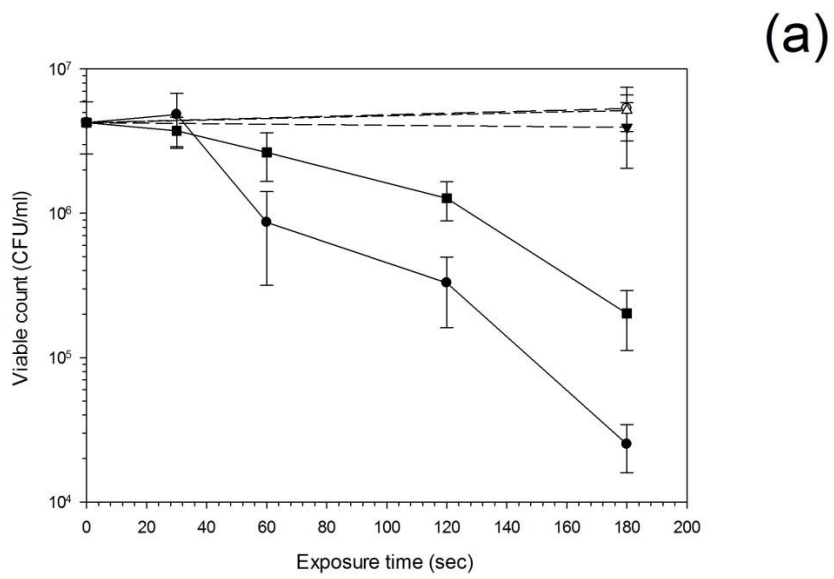


Figure 5

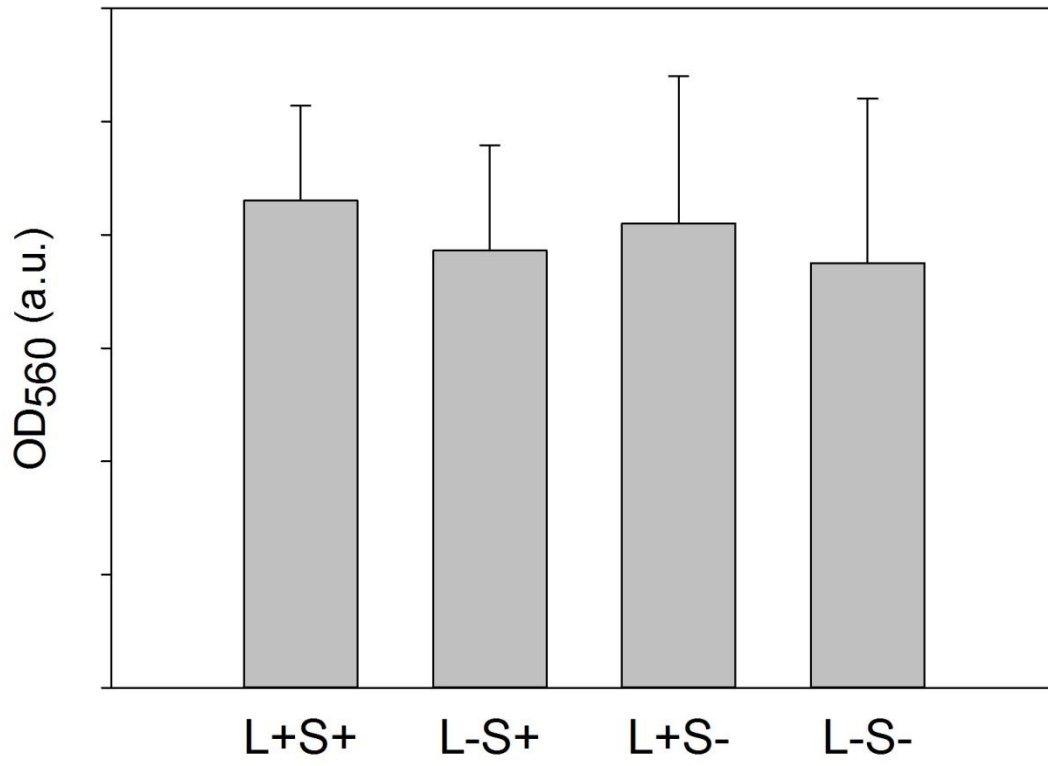


Figure 6

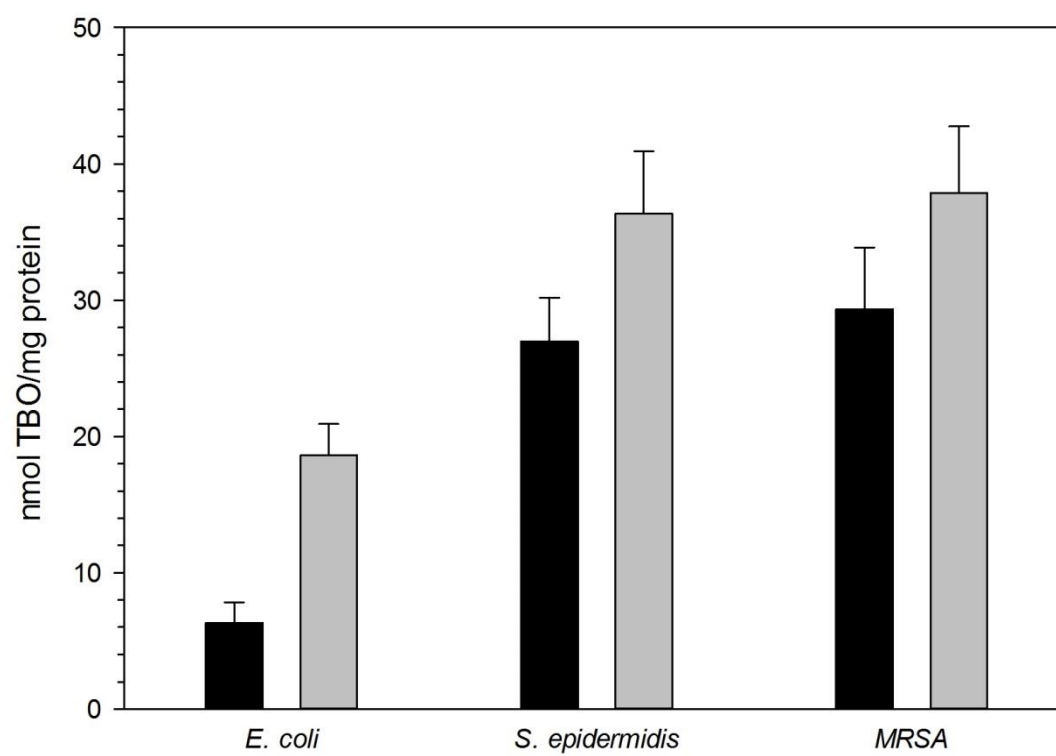


Figure 7

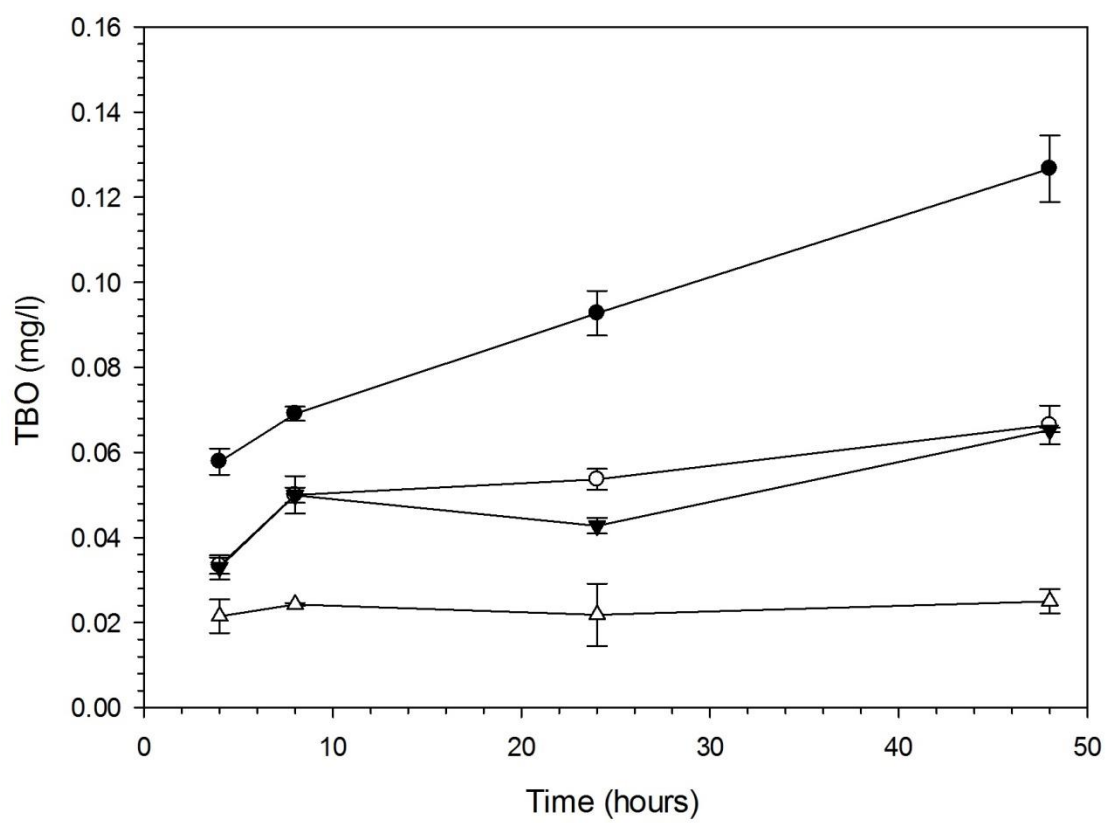


Figure 8